

## Time-Averaged Three-Dimensional Density and Temperature Field Measurement of a Turbulent Heated Jet Using Background-Oriented Schlieren

S. Amjad, J. Soria and C. Atkinson

Laboratory for Turbulence Research in Aerospace and Combustion  
 Department of Mechanical and Aerospace Engineering  
 Monash University, Victoria 3800, Australia

### Abstract

Three-dimensional time-averaged density and temperature fields of a heated air jet from a circular 10 mm diameter nozzle are reconstructed using tomographic background-oriented schlieren. A hybrid filtered back-projection–algebraic reconstruction (FBP-ART) technique reconstructs the refractive index gradient field in the flow. The number of ART iterations is varied to observe the effect on reconstruction artefacts. The largest improvement is observed after 1 ART iteration with filtering of the initial FBP solution. Subsequently, the gradient field is used to form a Poisson equation solved in a quasi-3D manner using successive over-relaxation. Convergence of the refractive index field is studied with iteration number and the effect this has on the temperature and density profiles, after applying the Gladstone-Dale relation and ideal gas law. The quasi-3D solution parallelises well, and converges rapidly.

### Introduction

Experimental investigation of flow structure dynamics in turbulent convective heat transfer has been hampered by the lack of robust methods for quantifying the instantaneous three-dimensional density and temperature fields. To study structures across a wide range of scales, ideally a non-intrusive measurement technique is needed. The background-oriented schlieren (BOS) technique, proposed by Raffel et al. [10], has shown much promise in this regard. BOS is an optical technique providing path-integrated estimates of the flow refractive index gradient field by imaging a background pattern while looking through the flow of interest. When performed from multiple angles around the flow, BOS provides a basis for tomographic reconstruction of the three-dimensional flow refractive index gradients. The refractive index field is then related to the flow density using the Gladstone-Dale relation. For an ideal gas, the temperature can be then be obtained using the ideal gas law, which provides scope for comparison with thermocouple measurements. Reconstruction of the gradient field from BOS data has been performed using Fourier transform-based filtered back-projection (FBP) [12] or the iterative algebraic reconstruction technique (ART) [2]. Further research is needed to evaluate and determine the optimal reconstruction methodology.

The current work serves as a preliminary study for a multiple-camera BOS system capable of obtaining instantaneous and time-averaged fields. Such a system is resource intensive, and it must be made certain that BOS and the tomographic reconstruction process could produce reliable results. First, the time-averaged density and temperature of a simple compressible flow will be considered. The ideal experimental and reconstruction parameters will be discovered. To achieve this, single-camera BOS is setup around a subsonic circular heated air jet with an exit temperature of 158 °C. This system can produce time-averaged 3D density and temperature fields equivalent to that produced by a multiple-camera setup. The flow is rotated to several azimuthal positions, with BOS performed at each position

to produce time-averaged inputs to the reconstruction method [1]. A hybrid FBP-ART approach, similar to Hartmann and Seume [4], reconstructs the gradient field, and an iterative solution of a Poisson equation formed from the gradients is applied to obtain the refractive index field. The effect of number of ART iterations on the strength of gradients is examined, especially in the context of computing time. The convergence of the Poisson solution is also examined. Application of the Gladstone-Dale relation and the ideal gas law to the refractive index field gives the density and temperature, respectively. This study acts as a proof-of-concept for a multiple-camera setup, giving some indication that any instantaneous fields produced with a multiple-camera setup are representative of true conditions. Conclusions are made on the effect of ART and Poisson solution iterations on the three-dimensional BOS reconstruction.

### Principles of tomographic background-oriented schlieren

BOS is based on the Gladstone-Dale relation between fluid density  $\rho$  and its refractive index  $n$

$$n - 1 = \rho G(\lambda), \quad (1)$$

where  $G(\lambda)$  is the Gladstone-Dale constant for incident light of wavelength  $\lambda$ . Originally an adaptation of speckle photography [8, 10], BOS capable of three-dimensional density measurements quickly emerged [12]. A camera and background are placed on either side of a flow. Images of the background through the flow appear distorted compared to ambient conditions, due to refractive index variations deflecting light rays travelling from the background to the camera. From figure 1, if the depth of the density variations is small compared to focal point-background distance  $Z_B$ , then light is approximately deflected by a path-integrated angle  $\epsilon$ , for both image directions  $x$  and  $y$ .

Digital cross-correlation of distorted and ambient images reveals an apparent displacement field  $\Delta$ ,

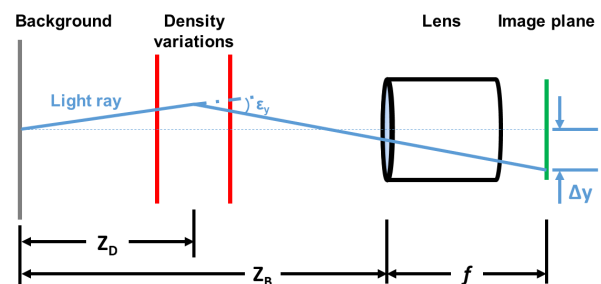


Figure 1: Optical setup for BOS demonstrating the apparent displacement of background features due to deflection of light rays by density gradients.

$$\Delta \approx \frac{\epsilon Z_D f}{Z_B}, \quad (2)$$

where  $f$  is the lens focal length and  $Z_D$  is the object-background distance. This provides a basis for quantitative measurement [10]. Multiple views of the flow enables tomographic reconstruction of the refractive index gradient field; for each view  $i$ , the deflections satisfy

$$\epsilon_{x_i} = \frac{1}{n_0} \int \frac{\partial n}{\partial x_i} dz_i, \quad (3)$$

with deflections in  $y_i$  also having the same form ( $n_0$  is the ambient refractive index). For three global orthogonal gradient components the refractive index field is determined by solving the Poisson equation

$$\frac{\partial^2 n}{\partial x^2} + \frac{\partial^2 n}{\partial y^2} + \frac{\partial^2 n}{\partial z^2} = q \quad (4)$$

where  $q$  is dependent on measured displacements and setup geometry. Application of equation 1 obtains a three-dimensional density field. Further, the ideal gas law can be applied for subsonic flows (knowing the pressure  $P$ ) to obtain a three-dimensional temperature field  $T$ . For instantaneous fields, projections must be recorded at the same time, which usually requires multiple cameras. A mean field could be recorded using a single camera, either moved around the flow, or is stationary with the flow rotated about an axis. It is imperative that the sensitivities and relative accuracies of experimental setups and reconstruction methods are first characterised with synthetic data [3], and then time-averaged data from single-camera measurements, before moving to multiple cameras.

### Tomographic reconstruction methods

Selection of a reconstruction methodology is not straightforward. Firstly, the refractive index field can be either obtained directly as done by Nicolas et al. [9] or by computing the gradient field and solving a Poisson equation [12]. The latter approach will be pursued in the current research. Further, there is a choice of gradient field reconstruction methods. Either filtered back-projection (FBP [6]) methods or algebraic reconstruction techniques (ART [5]) are used, and hybrid approaches have been tried as well [4]. FBP reconstructs gradients by taking the inverse Radon transform of sinograms which contain information about the sum of gradient components at each point in each view from the deflection information. It is a very efficient method, but significant reconstruction artefacts appear as the number of views lessens. ART is an iterative technique that starts with an initial solution to the gradient field, and corrects the solution by comparing the deflection of light rays through the solution against those required to produce the measured displacements. This is often much slower than FBP however reconstruction artefacts can be suppressed through judicious filtering. Hybrid approaches use the FBP reconstruction as the initial solution to the ART, producing equivalent solutions to ART alone with less iterations.

The hybrid approach was tested on synthetic data by Atkinson, Amjad and Soria [3], and will be used here on experimental data. The FBP reconstruction is applied within a cylindrical mask encompassing the jet, within a larger rectangular prism domain with ambient regions; this approach limits reconstruction artefacts. In addition to the ART, techniques which increase reconstruction quality in synthetic data are applied. These include randomising the order of views and light rays considered

for reconstruction and using a Hamming window filter on light ray path corrections which decreases the magnitude of corrections outside the jet (the beginning and end of the ray) and emphasising the correction inside the jet [6], and gradual unmasking restricting the severity of corrections per iteration [7].

### Experimental setup

Figure 2 shows the current setup for single-camera tomographic BOS of a heated air jet from a circular nozzle (diameter  $D = 10$  mm). The setup is detailed in Amjad, Soria and Atkinson [1]. A turntable allows rotation of the nozzle to  $1^\circ$ .

A DO3THINK M2ST120M camera (pixel size  $3.75 \mu\text{m}$ ) is placed  $500$  mm on one side of the jet, with the background equidistant on the other. From equation 2, a longer focal length results in larger displacements, and hence a higher signal-to-noise ratio. However, there are two conflicting requirements. Firstly, geometric blur

$$d_i = \frac{f}{N} \frac{f}{Z_D} \left(1 - \frac{Z_D}{Z_B}\right) \quad (5)$$

is the spatial averaging due to the out-of-focus jet placed between the camera and background (where  $N$  is the  $f$ -number). Cross-correlation already averages over window regions to find displacements; blur can be kept smaller than this to minimise additional uncertainty. Secondly, the diffraction-limited size

$$d_d = 2.44N \left(\frac{f}{Z_B} + 1\right) \lambda \quad (6)$$

is the smallest feature that can be imaged. For heated jets at  $160^\circ\text{C}$ , a  $50$  mm focal length at  $f/8$  is a good compromise between the three requirements [1]. Table 1 shows the selected BOS setup. The background pattern uses clear (backlit) spots in a semi-random pattern printed on a black background [10]. A pulsed LED ( $\lambda = 532$  nm) light exposes images for  $50 \mu\text{s}$  at  $8$  Hz. Settings for cross-correlation are summarised in table 2.

Parameter	Value
Object-background distance $Z_D$ (mm)	500
Focal point-background distance $Z_B$ (mm)	1000
Focal length $f$ and $f$ -number $N$ (mm)	50 at $f/8$
Background resolution ( $\mu\text{m}/\text{px}$ )	64.95
Object resolution ( $\mu\text{m}/\text{px}$ )	30.4
Geometric blur at background $d_i$ (px)	4.8
Diffraction-limited size at background $d_d$ (px)	0.2

Table 1: BOS parameters

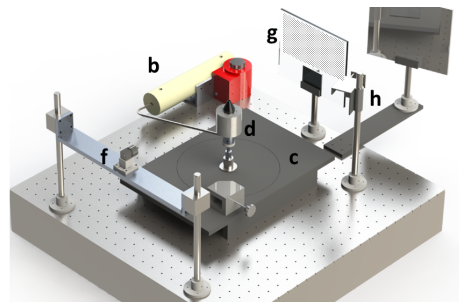


Figure 2: Experimental setup. a) Pressure regulator and heater; b) Turntable; c) Settling chamber and nozzle; d) Camera; e) Background and mirror; f) Pulsed LED and optics.

Parameter	Value
Image marker size (px)	2
Markers per window	10
Cross-correlation window size (px)	16 × 16
Window overlap (%)	75

Table 2: Cross-correlation parameters

The jet at 158 °C exit temperature is imaged at 15 positions spaced 12° apart, with 1500 images per position. This represents a typical multiple-camera BOS setup. Images are cross-correlated with a common reference image of the background in ambient conditions, producing displacement fields. The fields at each position are averaged, leaving 15 fields used for tomographic gradient field reconstruction. For the hybrid FBP-ART approach, the number of ART iterations is varied from 0 (FBP only) to 3. The Poisson solution is performed in a quasi-3D manner with successive over-relaxation; discrete transverse planes ( $x-z$ ) are solved independently along the streamwise direction  $y$ . Parallelisation is easily achieved: planes are solved by separate processors and collated afterwards. With inflow and outflow from the top and bottom faces of the reconstruction domain, the only boundary conditions required by this approach are at the sides, far outside the jet. These boundaries take on a fixed, known refractive index value. Iteration number is varied to study solution convergence.

## Results and discussion

Figure 3 illustrates an averaged displacement field (flow from bottom to top), with 210 vectors horizontally and 236 vertically. The direction indicates a positive temperature gradient. There are no transverse ( $\Delta x$ ) displacements far outside the jet and in the core near the nozzle due to constant temperature (within the measurement sensitivity of 0.1 px). Natural convection from the nozzle's top edge cause large longitudinal displacements there. These displacements are inputs to the tomographic reconstruction of the three-component refractive index gradient field.

Figure 4 compares the FBP and hybrid reconstructions. The FBP solution fluctuates greatly compared to the filtered hybrid solution, even towards the (ambient) boundaries. These are the reconstruction artefacts. Pre-filtering the ART iterations does much to remove these; the greatest improvement is seen in the first iteration with relatively little change thereafter. Fluctuating gradients in the core remain even with further iterations; there should be no gradients in this region. The FBP solution takes minutes on a workstation PC, while an ART iteration can take a few days (although the code is not optimised). A coarser vector spacing could also be used to improve this, and may still be as accurate. Given the minor improvement further iterations bring, it is reasonable that whole-field reconstructions may be sufficiently represented by FBP and one ART iteration.

Following gradient field reconstruction, the Poisson solution exhibits strong convergence, with an exponential decay in the RMS error between iterations relative to 10,000 iterations. By 5,000 iterations the error, normalised by the peak difference in the 10,000 iteration case, is 0.4% (figure 5). The RMS error of the entire field is less than 0.1% for 5000 iterations. This is an ideal compromise between computation time and convergence. The boundary condition is set to 1 as a placeholder, the field can be linearly offset to match experiment conditions. A boundary value of 1.000272 is chosen, for air at 20 °C, 101.325 kPa pressure and 60% humidity with  $\lambda = 532\text{nm}$  [11].

Applying equation 1 ( $G(\lambda) = 2.2598 \times 10^{-4} \text{m}^3/\text{kg}$ ) obtains the density field in figure 6. The axial banding of figure 6a is due to the quasi-3D approach exaggerating the refractive in-

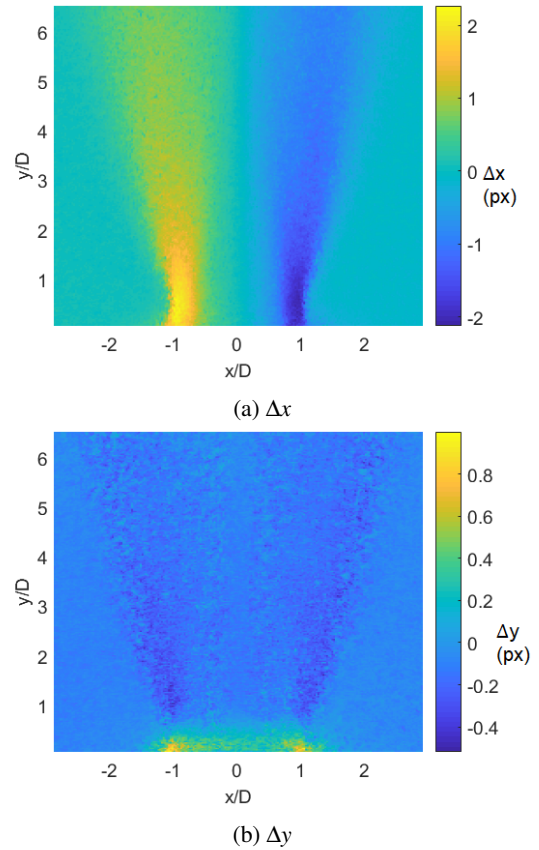


Figure 3: Transverse (a) and longitudinal (b) average displacements. Colourbar units in pixels, where 1 px = 64.95  $\mu\text{m}$ .

dex gradients along that direction; a full 3D solver may have a smoother solution. From the ideal gas law ( $R = 0.287\text{kJ}/(\text{kgK})$  and  $P = 101.325\text{kPa}$ ) the temperature range of the BOS solution with ART iterations is seen in figure 7 for 2500 Poisson solution iterations. A 3D view of a (cooler) ART reconstruction appears in figure 8. The FBP fluctuates in the jet core, and even in the ambient region. The ART and filtering reduces the fluctuations, however they are still noticeable. Further iteration increases the temperature, with a mean difference of 0.01% (maximum 4%) between 1 and 2 iterations.

## Conclusions

The hybrid FBP-ART refractive index gradient field reconstruction method is an efficient method of tomographic reconstruction of BOS data. The use of filters in ART following a single iteration allows reconstruction artefacts to be reduced, however the use of further ART iterations may bring negligible benefit. The Poisson equation solution for the refractive index field is sensitive to the number of iterations, with the field considered to be converged after 10000 iterations for the current case; within 5000 iterations, the global RMS difference with 10000 iterations is less than 0.1%. This may be a reasonable compromise between computation and accuracy. Further work should focus on the effect of adjusting filtering to reduce the impact of reconstruction artefacts, the effect of vector spacing, and a comparison with thermocouple measurements should be carried out to characterise the observed spatial fluctuations relative to another time-averaged temperature measurement approach.

## Acknowledgements

The authors acknowledge the Australian Research Council's (ARC) support. Dr. Atkinson was supported by the ARC Dis-

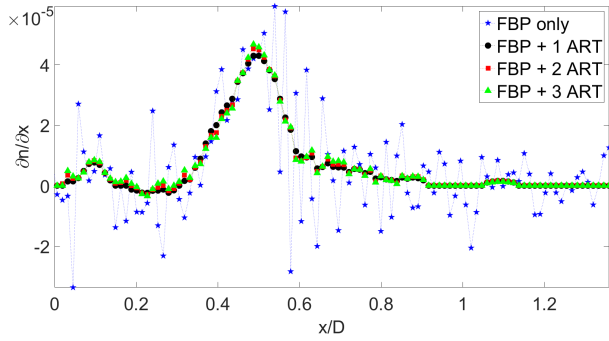


Figure 4: Comparison of FBP and hybrid approach with iteration number for  $\frac{\partial n}{\partial x}$  gradient at  $y/D = 0.1$  and  $z/D = 0$ .

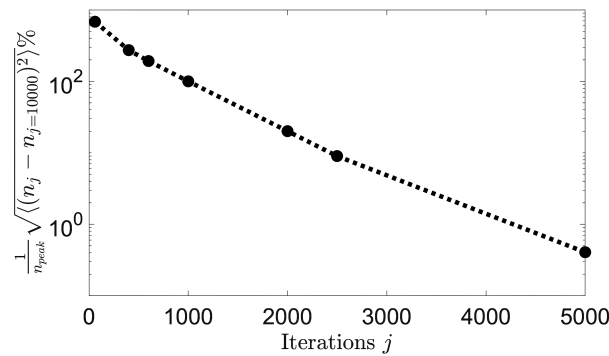
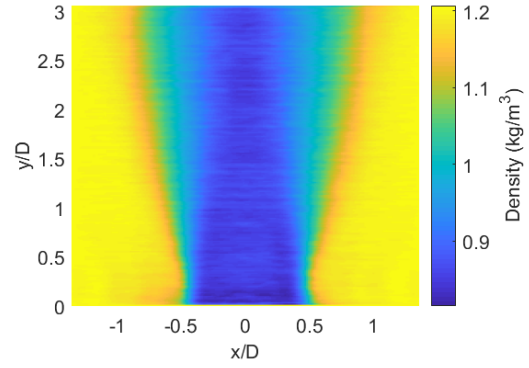


Figure 5: RMS error of Poisson solution with iteration number  $j$  relative to  $j = 10000$  iterations for  $y/D = 0.1$  and  $z/D = 0$ .

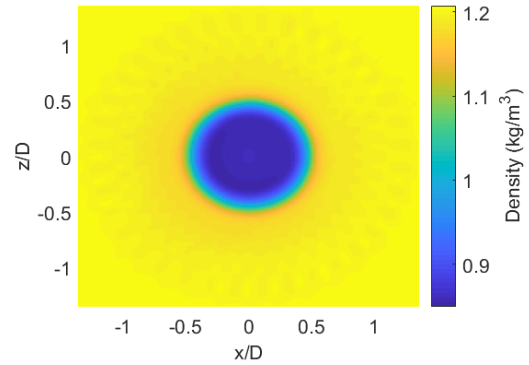
covery Early Career Researcher Award (DECRA) fellowship.

## References

- [1] Amjad, S., Soria, J. and Atkinson, C., Three-dimensional measurement of density and temperature in a turbulent heated jet, in *Proceedings of the 11th Australasian Heat and Mass Transfer Conference*, Melbourne, 2018.
- [2] Atcheson, B., Ihrke, I., Heidrich, W., Tevs, A., Bradley, D., Magnor, M. and Seidel, H.-P., Time-resolved 3D capture of non-stationary gas flows, in *ACM Transactions on Graphics*, 2008, volume 27.
- [3] Atkinson, C., Amjad, S. and Soria, J., A tomographic background-oriented schlieren method for 3D density field measurements in heated jets, in *Proceedings of the 11th Asia-Pacific Conference on Combustion*, Sydney, 2017.
- [4] Hartmann, U. and Seume, J. R., Combining ART and FBP for improved fidelity of tomographic BOS, *Measurement Science and Technology*, **27**, 2016, 097001.
- [5] Herman, G. T. and Lent, A., Iterative reconstruction algorithms, *Computers in Biology and Medicine*, **6**, 1976, 273–294.
- [6] Kak, A. C. and Slaney, M., *Principles of Computerized Tomographic Imaging*, Classics in Applied Mathematics, SIAM, Philadelphia, 2001.
- [7] Liao, H. Y., A gradually unmasking method for limited data tomography, in *2007 4th IEEE International Symposium on Biomedical Imaging: From Nano to Macro*, Arlington, VA, USA, 2007.



(a)  $x - y$  plane at  $z/D = 0$



(b)  $x - z$  plane at  $y/D = 0.75$

Figure 6: Longitudinal (a) and transverse (b) density field.

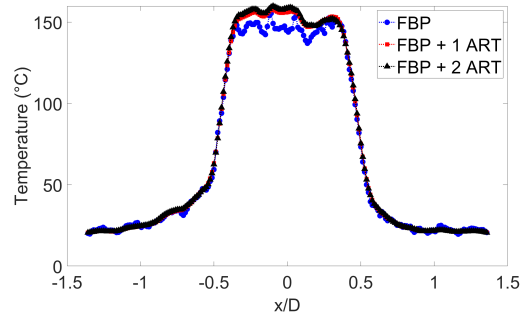


Figure 7: Temperature profile at  $y/D = 0.1$  and  $z/D = 0$  with varying ART iteration number.

- [8] Merzkirch, W., Density-sensitive whole-field flow measurement by optical speckle photography, in *Experimental Thermal and Fluid Science*, 1993, volume 7.
- [9] Nicolas, F., Todoroff, V., Plyer, A., LeBesnerais, G., Donjat, D., Micheli, F., Champagnat, F., Cornic, P. and LeSant, Y., A direct approach for instantaneous 3D density field reconstruction from background-oriented schlieren (BOS) measurements, *Experiments in Fluids*, **57**, 2015, 1–21.
- [10] Raffel, M., Richard, H. and Meier, G. E. A., On the applicability of background oriented optical tomography for large scale aerodynamic investigations, *Experiments in Fluids*, **28**, 2000, 477–481.
- [11] Stone, J. A. and Zimmerman, J. H., *Index of Refraction of Air*, National Institute of Standards and Technology, 2011.
- [12] Venkatakrishnan, L. and Meier, G. E. A., Density measurements using the background oriented schlieren technique, *Experiments in Fluids*, **37**, 2004, 237–247.

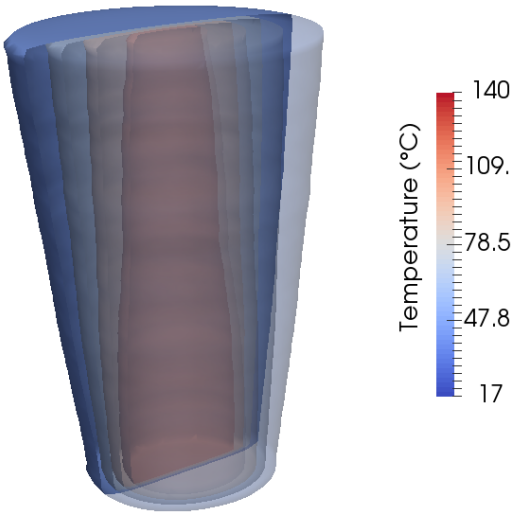


Figure 8: Three-dimensional temperature contours of an ART reconstructed jet.